Microstructural Dynamics of a Homopolymer Melt Investigated Using Two-Dimensional Raman Scattering

Kelly Huang, Lynden A. Archer, and Gerald G. Fuller*

Department of Chemical Engineering, Stanford University, Stanford, California 94305-5025

Received May 30, 1995; Revised Manuscript Received October 23, 1995[⊗]

ABSTRACT: The microstructural dynamics of polyisobutylene have been investigated using a new rheooptical technique, two-dimensional Raman scattering (2D Raman). 2D Raman employs intrinsic bond vibrations to selectively resolve the segmental dynamics within a material subjected to small-amplitude oscillatory deformation. In addition, interspecies interactions are probed through a cross-correlation of the orientation-induced response from distinct Raman peaks. It has been observed that the motions of the main chain and side groups in polyisobutylene are affected independently as the mechanical frequency is increased from the rubbery plateau into the glassy regime. In particular, at low frequencies (<10 s^{-1}) and room temperature, the motions of the side group and main chain are highly cooperative; however, at higher frequencies (>10 s^{-1}), the groups reorient independently as the mechanical glass transition is approached. The results are in accord with the observed frequency dependence of the stress-optical coefficient.

1.0. Introduction

An important aspect concerning the prediction of the rheology of multicomponent polymer systems is a fundamental understanding of the orientational evolution of individual constituents. Experimental methods such as mechanical rheometry and flow birefringence provide information of only bulk behavior and cannot selectively resolve segmental dynamics of a given species within a multicomponent system. For this reason, spectroscopic methods, such as Raman and infrared, have been employed. This paper presents a new technique based on Raman scattering that has been developed to exploit intrinsic bond vibrations to probe constituent dynamics. As demonstrated in this study, the terms constituent and component are general and include different functional groups on the same polymer chain.

Raman scattering has been utilized in the past by several groups to characterize orientation in polymers.[1] However, these conventional techniques mandate the manual manipulation of the polarization state of light and, therefore, are not amenable to performing dynamic experiments. Recently, Archer, Fuller, and Nunnelley introduced photoelastic modulation to Raman scattering in order to automate the change of polarization,[2] thus alleviating this limitation. Subsequently, Archer, Huang, and Fuller utilized polarization-modulated laser Raman scattering (PMLRS) to successfully monitor the relaxation dynamics of polyisobutylene following step elongation.[3] In that study, Archer and co-workers, for the first time, measured the time-dependent second and fourth moments of the polymer orientation distribution function to compare the validity of several molecular rheological models. The current work introduces an extension of the PMLRS experiment, two-dimensional Raman scattering, or 2D Raman.

This paper describes the principles and molecular basis of 2D Raman. Unlike the PMLRS experiment, which quantifies the magnitudes of the second and fourth moments, 2D Raman monitors the deformation-induced response of these moments to an oscillatory flow field. The orientation measure introduced is the *Raman anisotropy*, which allows for viscoelastic characterization of a particular species within a polymer system. Furthermore, by incorporating a simultaneous birefringence measurement, 2D Raman probes bulk dynamics as well.

By comparing the molecular description of the stress, a stress−Raman rule is derived to relate the Raman anisotropy of a particular component to the stress borne by that component. In addition to the ability to measure individual component viscoelasticity, 2D Raman provides a measure of interspecies interactions through cross correlation of the Raman anisotropy emanating from distinct constituents. This use of cross correlation techniques with vibrational spectroscopy was first proposed by Noda in the development of two-dimensional infrared spectroscopy (2DIR).[4,5] Although both Raman and infrared provide similar physical information, the Raman-based experiment offers many advantages with respect to multicomponent polymer rheology. For instance, the ability to use monochromatic excitation and to use glass sample windows yields simplicity in calibration and sample handling. Moreover, as opposed to infrared absorption, Raman scattering measurements offer experimental flexibility in that they are not limited to thin films and can be used to study solutions.

It should be noted that recent studies have introduced techniques also referred to as two-dimensional Raman.[6,7] However, these studies differ from the current in both scope and instrumentation. Ebihara, Takahashi, and Noda[6] investigate the nanosecond time regime, and Gustafson *et al.*[7] study the picosecond time regime following photoexcitation by cross correlation of resonance Raman spectra obtained using the conventional pump−probe method. These studies elicit information regarding the change in peak intensity due to the transient lifetime of photoexcited molecules. In contrast, the current study quantifies the change in submolecular orientation due to the application of an oscillatory flow. Nonresonance, polarization-modulated Raman scattering is utilized, and a new orientation measure, the Raman anisotropy, is cross correlated. In particular, a study of the microstructural dynamics in polyisobutylene is presented. 2D Raman has the selectivity and resolution to separately monitor the reorientation of the methyl side groups independent of the main chain at room temperature. It is observed that, at flow frequencies above 10 s^{-1}, there is a slight difference in

[⊗] Abstract published in *Advance ACS Abstracts,* January 1, 1996.

0024-9297/96/2229-0966$12.00/0

the motions of the main chain and side groups. This suggests a mechanism by which the stress-optical coefficient for polyisobutylene becomes dependent on strain frequency as the mechanical glass transition is approached.

2.0. Background

2.1. Raman Scattering. The nature of the Raman effect involves transitions of vibrational states, and therefore, a thorough treatment necessitates quantum mechanics. However, for this work, classical electromagnetic theory is sufficient and predicts the pertinent results that are unaltered when quantum considerations are introduced. For a rigorous description of Raman spectroscopy, the reader is referred to the book by Long.[8]

As in the case of Rayleigh scattering, Raman scattering is a result of the interaction of light with an induced oscillating dipole. For normal Raman and Rayleigh scattering, the induction of a dipole moment, P_i, related to an electric field with amplitude E^o_j and frequency ν_o is given by

$$P_i = \alpha_{ij} E^o_j \cos(\nu_o t) \tag{1}$$

where α_{ij} is the polarizability tensor.

In general, the polarizability will be a function of the nuclear coordinates; therefore, the variation of the polarizability with vibrational mode k can be expressed as a Taylor series expansion with respect to the normal coordinate of vibration, Q_k, associated with vibrational frequency ν_k. To first order in Q,

$$\alpha_{ij} = \alpha^o_{ij} + \alpha'_{ij} \cos(\nu_k t + \delta_k) \tag{2}$$

where δ_k is a phase shift and $\alpha'_{ij} = (\partial\alpha_{ij}/\partial Q_k)Q_k$ is the derived polarizability tensor or Raman tensor.

Substitution of eq 2 into eq 1 demonstrates that radiation oscillating with a frequency ν_o will induce a dipole that radiates with three components: $P_i(\nu_o)$ or Rayleigh scattering arising from the average polarizability tensor, α^o_{ij}; $P_i(\nu_o+\nu_k)$ or anti-Stokes Raman scattering; and $P_i(\nu_o-\nu_k)$ or Stokes Raman scattering. The intensity of the Raman scattered light is given by

$$I = I_o \langle (n^o_i \alpha'_{ij} n^s_j)^2 \rangle \tag{3}$$

where I_o is the incident light intensity, n^o_i and n^s_j are unit vectors describing the polarization of the incident and scattered light, and the angled brackets denote an average about the orientation distribution of scatterers. In general, α'_{ij} is a function of the orientation of individual scattering elements within the sample; thus, the Raman scattered intensity contains information regarding the average orientation within the system.

2.2. Cartesian Analysis of the Raman Tensor. The relation of the Raman scattered intensity to polymer orientation was first established by Bower through a spherical harmonic expansion of the Raman tensor.[9] However, recently Archer, Huang, and Fuller performed a generalized tensor analysis of the derived polarizability tensor in order to relate the Raman scattered intensity to Cartesian moments of the orientation distribution function.[3] This Cartesian analysis, as opposed to the harmonic expansion in the Euler angles, provides a convenient representation for investigating rheology since it allows for a more direct comparison of the polarized Raman intensity to elements of the stress tensor.

The analysis of Archer and co-workers treats the derived polarizability tensor analogously to the treatment of the polarizability tensor for strained polymers.[10] However, in contrast to strain birefringence, eq 3 shows that the intensity of Raman scattered light necessitates the treatment of the fourth-order tensor, $\langle \alpha'_{ij}\alpha'_{kl} \rangle$. In this Kuhn–Grün method, the polymer molecule is idealized as a hypothetical chain of n traversely-isotropic, randomly-jointed links of length b. Moreover, it is shown that the quadratic Raman tensor can be related to the orientation of these random links as follows:

$$\begin{aligned}\langle \alpha'_{ij}\alpha'_{kl} \rangle = {} & \left(\alpha'^2_2 + \frac{B^2}{8} + \alpha'_2 B\right)\delta_{ij}\delta_{kl} + \\ & \frac{B^2}{8}(\delta_{ik}\delta_{jl} + \delta_{il}\delta_{jk}) + \\ & \left(\alpha'_2 A - \frac{B^2}{8} - \frac{\alpha'_2 B}{2} + \frac{AB}{2}\right)\{\delta_{kl}\langle r_i r_j \rangle + \delta_{ij}\langle r_k r_l \rangle\} + \\ & \left(\frac{C^2}{2} - \frac{B^2}{2}\right)\{\delta_{jl}\langle r_i r_k \rangle + \delta_{il}\langle r_j r_k \rangle + \delta_{ik}\langle r_j r_l \rangle + \delta_{jk}\langle r_i r_l \rangle\} + \\ & \left(A^2 + \frac{3B^2}{8} - 2C^2 - AB\right)\langle r_i r_j r_k r_l \rangle \end{aligned} \tag{4}$$

where r_i is the unit vector defining statistical segment orientation, $A = (\alpha'_1 - \alpha'_2)\cos^2\theta + (\alpha'_3 - \alpha'_2)\sin^2\theta$, $B = (\alpha'_1 - \alpha'_2)\sin^2\theta + (\alpha'_3 - \alpha'_2)\cos^2\theta$, and $C = (\alpha'_1 - \alpha'_3)\sin\theta\cos\theta$. Here, α'_1, α'_2, and α'_3 are the eigenvalues of the Raman tensor, θ is the angle between r_i and the principal frame, and δ_{ij} is the identity tensor. It can be shown that converting eq 4 to spherical coordinates results in a representation of the Raman tensor that is identical to the one developed for liquid crystals.[11]

Furthermore, Kuhn and Grün showed that the statistical distribution of link angles can be defined if the number of links is large.[12] Therefore, the mean components of the quadratic Raman tensor for the chain may be obtained. Archer and co-workers showed that in this representation, the quadratic Raman tensor can be related to the orientation of end-to-end vectors, R_i, through the following relationships:

$$\langle r_i r_j \rangle = \left\{\frac{1}{3} - \frac{1}{5}\left(\frac{R}{N_K a}\right)^2 - \frac{12}{175}\left(\frac{R}{N_K a}\right)^4\right\}\delta_{ij} + \left\{\frac{3}{5}\left(\frac{1}{N_K a}\right)^2 + \frac{36}{175}\frac{R^2}{(N_K a)^4}\right\}R_i R_j$$

$$\begin{aligned}\langle r_i r_j r_k r_l \rangle = {} & \left\{\frac{1}{15} - \frac{2}{35}\left(\frac{R}{N_K a}\right)^2 - \frac{3}{175}\left(\frac{R}{N_K a}\right)^4\right\}(\delta_{ij}\delta_{kl} + \delta_{ik}\delta_{jl} + \delta_{il}\delta_{jk}) + \\ & \left\{\frac{3}{35}\left(\frac{1}{N_K a}\right)^2 + \frac{3}{175}\frac{R^2}{(N_K a)^4}\right\}(\delta_{ij}R_k R_l + \delta_{kl}R_i R_j + \\ & \delta_{ik}R_j R_l + \delta_{jk}R_i R_l + \delta_{il}R_j R_k + \delta_{jl}R_i R_k) + \\ & \frac{3}{35}\left(\frac{1}{N_K a}\right)^4 (R_i R_j R_k R_l) \end{aligned} \tag{5}$$

for a chain of N_K links of length a.

2.3. The Raman Anisotropy. Equation 3 describes the Raman intensity from a scattering element given that the polarization of the incident and scattered light

are known. However, in the case of strained polymers, the polarization characteristics of the exciting and resulting Raman scattered radiation are affected by birefringence, which alters the phase of the light as a result of segment orientation. In order to account for this phenomenon, Archer, Fuller, and Nunnelley present a rigorous, Jones−Mueller matrix treatment of Raman scattering within a birefringent medium.[2] A result of this analysis is the identification of an element of the sample's Mueller matrix that is a measure of preferential orientation. Specifically, this measure is introduced here as the *Raman anisotropy*, $\Gamma(\nu)$, and is mathematically defined as

$$\Gamma(\nu) = \langle \alpha'_{xx}{}^2 \rangle - \langle \alpha'_{zz}{}^2 \rangle \tag{6}$$

Here, x is the flow direction and light propagates along the y-axis. By substitution of eq 4 into eq 6, it is evident that $\Gamma(\nu)$ measures the anisotropy in the second and fourth moments of the distribution function describing the orientation of statistical segments or end-to-end vectors. In general, the Raman anisotropy is of the form

$$\Gamma(\nu) = \gamma_1(\nu)(\langle x^2 \rangle - \langle z^2 \rangle) - \gamma_2(\nu)(\langle x^4 \rangle - \langle z^4 \rangle) \tag{7}$$

where γ_1 and γ_2 are constants defined by the substitution. As stated earlier, 2D Raman utilizes an oscillatory sample deformation; therefore, it is expected that the Raman anisotropy yields an oscillatory response.

2.4. Stress−Raman Relationship. The basic principle underlying the ability to optically probe polymer rheology is that both the stress and optical anisotropy are a consequence of segmental orientation. A familiar result of this coupling is the stress-optical rule for Gaussian chains. The stress-optical law states that the refractive index tensor is proportional to the stress tensor.[13] A similar relation can be obtained for the proportionality of the stress to the dynamic Raman anisotropy for a sample undergoing small-amplitude oscillatory perturbation.

The stress−Raman rule can be demonstrated by considering molecular models of polymer dynamics. To demonstrate this principle, two fundamental models are considered: the elastic dumbbell model for dilute solutions and the temporary network model for entangled melts.[13,14] Since these are molecular theories, they incorporate a Smoluchkowski equation of continuity for the distribution function, ψ, describing the orientation of end-to-end vectors. From the Smoluchowski equation, equations of motion for the second, $\langle r_i r_j \rangle$, and fourth, $\langle r_i r_j r_k r_l \rangle$, moments of the orientation distribution function can be derived. To first order in the small-amplitude oscillatory extension, $\epsilon = \epsilon^o \sin(\omega t)$, the dumbbell and temporary network models yield the following equations for the evolution of $\langle x^2 \rangle - \langle z^2 \rangle$ and $\langle x^4 \rangle - \langle z^4 \rangle$:

$$\langle x^2 \rangle - \langle z^2 \rangle = 3\epsilon^o \frac{\lambda^2\omega^2}{1+\lambda^2\omega^2} \sin(\omega t) + 3\epsilon^o \frac{\lambda\omega}{1+\lambda^2\omega^2} \cos(\omega t)$$

$$\langle x^4 \rangle - \langle z^4 \rangle = 2(\langle x^2 \rangle - \langle z^2 \rangle) \tag{8}$$

Here, λ is the longest relaxation time for the temporary network model, and $\lambda = \zeta/8kT\beta^2$ for the dumbbell model, where ζ is the friction coefficient, k is Boltzmann's constant, and $\beta^2 = 3/2N_K a^2$ contains the constants of the Kuhn and Grün statistical chain. Comparing eq 8 to the molecular description of the normal stress,[14] $\sigma_{xx} - \sigma_{zz} = 2kT\rho\beta^2(\langle x^2 \rangle - \langle z^2 \rangle)$, it can be seen that the stress and Raman anisotropy are related by $C_\Gamma = [\gamma_1(\nu) - 2\gamma_2(\nu)]/2kT\rho\beta^2$, the stress−Raman constant for the component emitting Raman scattered light at wavenumber ν. Here, ρ is the number of chains per unit volume.

By substituting the solutions, eq 8, into eq 7, the Raman anisotropy becomes a dynamic Raman anisotropy, $\tilde{\Gamma}$:

$$\tilde{\Gamma}(\nu) = \epsilon^o\{\Gamma'(\nu)\sin(\omega t) + \Gamma''(\nu)\cos(\omega t)\} \tag{9}$$

where $\Gamma'(\nu)$ and $\Gamma''(\nu)$ are the in-phase and out-of-phase components of the dynamic Raman anisotropy, respectively. $\Gamma'(\nu)$ and $\Gamma''(\nu)$ define Raman-based analogs to the storage and loss moduli of mechanical rheometry. Written in terms of the amplitude, Γ^o, of the dynamic Raman anisotropy and the phase angle, δ, between $\tilde{\Gamma}$ and the strain,

$$\tilde{\Gamma}(\nu) = \Gamma^o(\nu)\sin(\omega t + \delta(\nu)) \tag{10}$$

Trigonometry defines $\Gamma' = (\Gamma^o/\epsilon^o)\cos(\delta)$, $\Gamma'' = (\Gamma^o/\epsilon^o)\sin(\delta)$, and $\tan(\delta) = \Gamma''/\Gamma' = 1/\lambda\omega$.

Thus, similar to birefringence, the Raman anisotropy provides a measure of the state of stress within the system. However, unlike birefringence, the Raman anisotropy isolates the stress borne by a particular species within the system. Therefore, 2D Raman has the capability to monitor the viscoelasticity of individual components within a multicomponent system.

2.5. Two-Dimensional Correlation Analysis. In addition to characterizing individual component viscoelasticity, 2D Raman provides for a measure of interspecies interactions. This is accomplished by cross correlating the dynamic Raman anisotropy arising from distinct constituents. The application of cross correlation analysis to spectroscopic measurements was first proposed by Noda in the development of 2DIR.[4,5] Equation 11 displays the limiting cross correlation of the dynamic Raman anisotropy emanating from the component containing bond vibration ν_1 and the component with bond vibration ν_2.

$$\chi(\tau) = \lim_{\eta\to\infty} \frac{1}{\eta}\int_{-\eta/2}^{\eta/2} \tilde{\Gamma}(\nu_1,t)\,\tilde{\Gamma}(\nu_2,t+\tau)\,\mathrm{d}t \tag{11}$$

where τ is the correlation time.

Substitution of eq 10 into eq 11 yields the solution

$$\chi(\tau) = \Phi(\nu_1,\nu_2)\cos(\omega\tau) + \Psi(\nu_1,\nu_2)\sin(\omega\tau) \tag{12}$$

$\Phi(\nu_1,\nu_2)$ is the synchronous correlation intensity

$$\Phi(\nu_1,\nu_2) = \frac{1}{2}\Gamma^o(\nu_1)\,\Gamma^o(\nu_2)\cos\{\delta(\nu_1) - \delta(\nu_2)\} \tag{13}$$

and $\Psi(\nu_1,\nu_2)$ is the asynchronous correlation intensity

$$\Psi(\nu_1,\nu_2) = \frac{1}{2}\Gamma^o(\nu_1)\,\Gamma^o(\nu_2)\sin\{\delta(\nu_1) - \delta(\nu_2)\} \tag{14}$$

Since $\Phi(\nu_1,\nu_2)$ is a maximum when $\delta_1 = \delta_2$, it is obvious that large values of the synchronous correlation intensity suggest simultaneous reorientation of the two components. On the other hand, $\Psi(\nu_1,\nu_2)$ is a maximum when the two species lag the strain exactly in quadrature with each other. Thus, large values of the asyn-

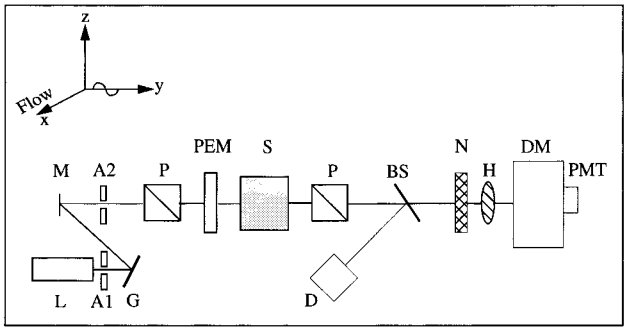

Figure 1. 2D Raman apparatus for simultaneous measurement of the Raman anisotropy and birefringence. The instrument consists of an argon ion laser (L), entrance aperture (A1), monochromator grating (G), mirror (M), exit aperture (A2), linear polarizers (P), photoelastic modulator (PEM), oscillatory flow cell (S), beam splitter (BS), notch filter (N), half-wave plate (H), double monochromator (DM), photomultiplier tube (PMT), and GaAs detector (D). Light propagates along the *y*-axis through the sample, which is undergoing oscillatory flow along the *x*-axis.

chronous correlation imply independent reorientation of the two constituents. As an example, a miscible blend would yield a large synchronous intensity and no asynchronous behavior since the components exhibit cooperative dynamics. However, in the case of an immiscible blend, the constituents retain much of their own dynamics; thus, an immiscible system would display a large asynchronous correlation intensity.

3.0. Experimental Section

3.1. Apparatus. Oscillatory extension is applied to the sample using a simple flow cell. The device is composed of a translation stage equipped with clamping fixtures and is driven by a servo motor that is commanded via a function generator. Motion control is provided by the servo amplifier that utilizes feedback from a rotational voltage displacement transducer attached to the motor shaft.

The 2D Raman optical train, Figure 1, is based upon the experimental apparatus developed for polarization-modulated laser Raman scattering.[2,3] An argon ion laser, operating at 100 mW, provides monochromatic light at 514.5 nm and propagates along the *y*-axis. The beam is passed through optics to remove plasma lines. These optics consist of an entrance aperture, monochromator grating, mirror, and exit aperture. Then, a polarizer establishes the polarization along the *x*-axis, and the polarization generating section is completed with a photoelastic modulator (PEM) oriented at 45° to the *x*-axis. The PEM modulates the polarization of the incident light by introducing a sinusoidal phase retardation at a frequency $f = 42$ kHz in the $x-z$ plane. The transmitted and Raman scattered light from the sample, undergoing flow along the *x*-axis, is collected with a lens and analyzed with a polarizer at 45° to the *x*-axis. A beam splitter is employed to partially reflect this light to a GaAs photodetector that simultaneously measures birefringence, and a notch filter eliminates the laser line so that the Raman scattered light intensity can be measured using a double monochromator and photomultiplier tube (PMT). Prior to the monochromator, a half-wave plate is employed to maximize the throughput by offsetting the polarization bias of the gratings.

Mechanical data used in the stress-optical comparison were obtained using a Rheometrics RDA II rheometer. Parallel plates with a diameter of 25 mm and a gap of 1−2 mm were utilized for the measurement.

3.2. Signal Analysis. Since the PEM introduces a sinusoidal retardation of the incident light, $\delta_{PEM} = p \sin(ft)$, the signals from the photodetector and PMT are of the form

$$\frac{I}{I_o} = R_{dc} + 2J_1(p)R_f \sin(ft) + 2J_2(p)R_{2f} \cos(2ft) \quad (15)$$

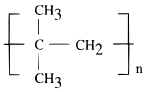

Figure 2. Repeat unit of polyisobutylene. Motions of the main chain and methyl side groups are investigated.

where I_o is the incident light intensity and $J_1(p)$ and $J_2(p)$ are Bessel function coefficients arising from the Fourier decomposition of the intensity signal.[2] The raw signals are amplified with low-noise current amplifiers and then demodulated using lock-in amplifiers and low-pass filters. For 2D Raman, the component of interest from the Raman scattered intensity measured by the PMT is R_{2f}, defined as follows for this optical arrangement:

$$R_{2f}(\nu) = \frac{1}{4}\tilde{\Gamma}(\nu) \quad (16)$$

The PMT dc signal is also collected to monitor possible extraneous intensity variations due to surface defects, sample thinning, etc. This component serves as a normalization of the $2f$ intensity signal even though it is also dependent on moments of the orientation distribution functions through the following relationship:

$$R_{dc}(\nu) = \frac{1}{8}\{\langle \alpha'_{xx}{}^2 \rangle + 2\langle \alpha'_{xz}{}^2 \rangle + \langle \alpha'_{zz}{}^2 \rangle\} \quad (17)$$

However, unlike the Raman anisotropy which is related to the difference in moments, the dc signal is related to the sum of moments. Thus, R_{dc} is fairly insensitive to the applied flow since a decrease in orientation along one coordinate results in an increase along another.

The photodetector, which simultaneously monitors the bulk orientation, provides a measure of the sample's birefringence in the form

$$R_f^{birf} = \sin(\delta') \quad (18)$$

where δ' is the retardation and is related to the birefringence, $\Delta n'$, by $\delta' = 2\pi\Delta n' d/\lambda$ for light of wavelength λ with path length d.

A computer equipped with an analog to digital board acquires the signals from the lock-in amplifiers and low-pass filters. The attenuation and roll-off effect of time constants and cut-off frequencies are corrected for using the equations from single pole filter theory.[15] Additionally, fast Fourier transforms are then utilized to quantify the amplitudes and phases relative to the applied strain and cross correlation analyses are performed.

3.3. Sample Preparation. The sample investigated is a polyisobutylene homopolymer provided by BASF and is of molecular weight $M_w = 300\,000$ and polydispersity $M_w/M_n = 2.8$ as characterized by GPC referenced to polystyrene. 2D Raman is utilized to monitor the dynamics of the main chain independent of the methyl side groups for polyisobutylene, whose structure is shown in Figure 2. Initially, the polymer is dissolved in toluene and reprecipitated in 2-propanol. It is then dried under vacuum for 48 h at 65 °C. Subsequently, the material is compressed in a glass-lined mold into dumbbell-shaped samples (25 × 8 × 4 mm) and annealed at 65 °C for 24 h. The resulting dumbbell is inspected between crossed polarizers in order to confirm the absence of residual stresses.

4.0. Results and Discussion

The polarized and depolarized Raman spectra of an isotropic, undeformed polyisobutylene sample are shown in Figure 3. Two highly polarized regions exist at approximately 700 and 2900 cm^{-1}. The low depolarization ratios of these Raman bands imply that they are highly sensitive to macroscopic orientation. The peak at around 2900 cm^{-1} is typical of the combination of the symmetric and asymmetric carbon−hydrogen modes in

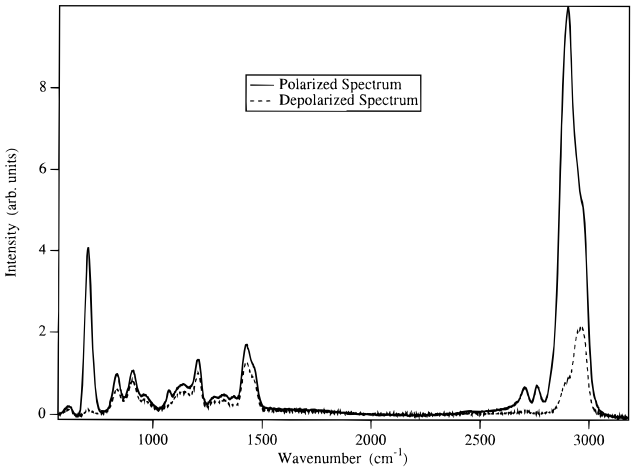

Figure 3. Raman spectra from an isotropic, nonstressed polyisobutylene sample. The solid curve represents the polarized spectrum, and the dashed curve represents the depolarized spectrum.

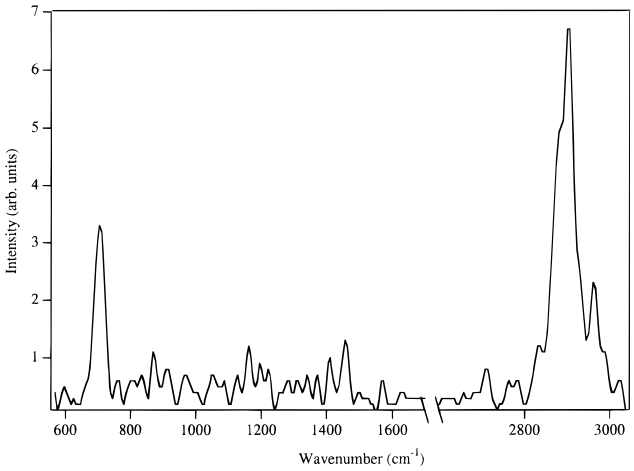

Figure 4. Raman anisotropy amplitude vs wavenumber for a polyisobutylene sample undergoing a 1.5% oscillatory extension at 82 s^{-1} and room temperature.

polymer systems,[8,16] and the band at 700 cm^{-1} is assigned to the methylene rocking mode, $\gamma_r(CH_2)$, which shows up as low-frequency peaks in the spectra of polymers such as polyethylene.[17,18] These two regions are used as "tags" to provide insight into the microstructural dynamics of polyisobutylene. With the application of an oscillatory extension, the dynamic Raman and birefringence signals are monitored and analyzed to determine the moduli and correlation intensities.

The amplitude, $\Gamma^o(\nu)$, of the Raman anisotropy in response to an 82 s^{-1}, 1.5% extension at room temperature is plotted against wavenumber in Figure 4. This plot exhibits the susceptibility of the vibrational groups to the applied deformation. The only noticeable features are the two peaks corresponding to the symmetric/asymmetric CH and $\gamma_r(CH_2)$ regions. It is interesting to note that the peaks between 700 and 1500 cm^{-1}, although they show significant intensity in the Raman spectrum, do not respond appreciably to the induced orientation. This is expected based upon the high depolarization exhibited by these bands in Figure 3 and is confirmation of the decoupling of the Raman R_{2f} term from birefringence as predicted by Mueller calculus.[2]

Figure 5 displays the Raman anisotropy moduli and birefringence moduli at 1.5% extension with frequency varying over 4 decades. As stated earlier, birefringence

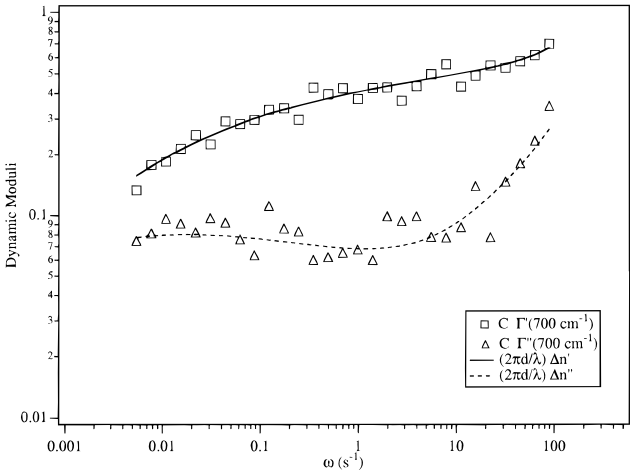

Figure 5. Frequency sweep of the Raman anisotropy moduli from the $\gamma_r(CH_2)$ peak at 700 cm^{-1} for a strain of 1.5% at room temperature superimposed onto the birefringence moduli by a single constant, *C*.

serves as a probe of bulk rheology, whereas the Raman anisotropy investigates bond-level dynamics. Since the polyisobutylene sample under consideration is a homopolymer, it is not surprising that the Raman anisotropy moduli are directly proportional to the birefringence moduli. It should also be noted that the Raman anisotropy from the $\nu_s(CH_3)$ overlaps with a different proportionality constant than the $\gamma_r(CH_2)$ depicted. While Figure 5 demonstrates the capability of 2D Raman to explore individual component rheology, Figure 6 illustrates the ability to probe interspecies interactions.

Cross correlation of the dynamic response of distinct peaks defines two independent wavenumbers and provides information regarding cooperative reorientation. In addition, as shown in Figure 6, cross correlation enhances spectral resolution since distinct functional groups may respond to the flow differently. For a 1.5% oscillatory extension at 82 s^{-1}, cross correlation improves the resolution of the symmetric/asymmetric CH profile. In particular, the symmetric CH stretch from the methyl side groups, $\nu_s(CH_3)$, at 2900 cm^{-1} and the asymmetric CH stretch from the polymer backbone, $\nu_a(CH_2)$, at 2926 cm^{-1} are resolved.[18] External to the plots in Figure 6 are the graphs of the regions corresponding to the correlation wavenumbers.

Figure 6a displays the synchronous component of the cross correlation. The contours along the diagonal represent the power spectrum of the dynamic Raman anisotropy. Intensity peaks off of the diagonal are referred to as cross peaks and suggest simultaneous reorganization of the functional group to the applied perturbation. For the homopolymer melt, it is not surprising that Figure 6a shows a high synchronous correlation between the symmetric/asymmetric CH and $\gamma_r(CH_2)$ reorientations.

Within the asynchronous spectrum, the only feature that appears above the noise level is a low-intensity cross peak within the symmetric/asymmetric CH Raman anisotropy profile. Figure 6b displays the asynchronous correlation spectrum in this region. Although the magnitude is much less than the synchrous correlation, the existence of an asynchronous intensity, Ψ(2900 cm^{-1}, 2926 cm^{-1}), reveals that there is a slightly different rate of reorientation of the CH bonds along the backbone and the CH bonds on the methyl side groups. Marcott and co-workers, using 2DIR, reported similar

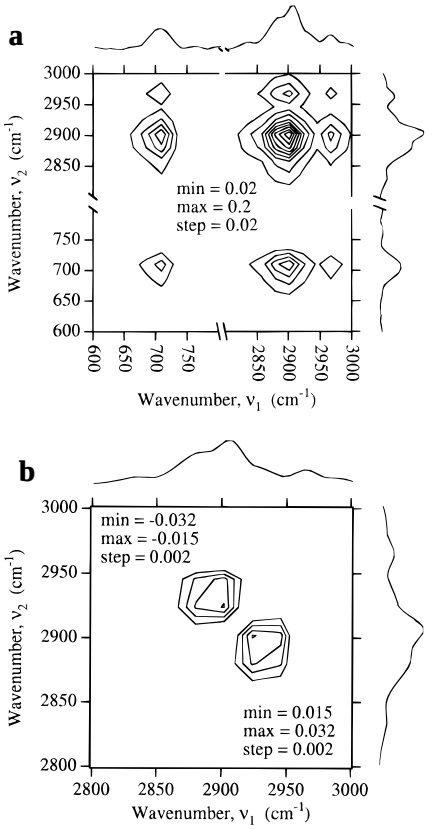

Figure 6. Cross correlation of the dynamic Raman anisotropy at various wavenumbers for a sample undergoing a 1.5% oscillatory extension at 82 s^{-1} and room temperature. Isointensity contours are plotted from a value *min* to a value of *max* by increments of *step*. (a) Synchronous correlation intensity. (b) Asynchronous correlation intensity within the symmetric/asymmetric CH profile.

asynchronicity between the phenyl side groups and the main chain in polystyrene.[19] However, the work on polystyrene was performed at room temperature, well below the glass transition temperature. Polyisobutylene, on the other hand, possesses a glass transition temperature of $T_g = -73$ °C and has sufficient mobility at room temperature.

To better understand this phenomenon, the peak intensity of the asynchronous correlation between the main chain and side groups is measured as a function of frequency. Figure 7 shows that, as expected, there is no asynchronous intensity at low frequencies. However, above approximately 10 s^{-1}, the absolute magnitude of the asynchronous intensity increases dramatically from zero. This increase in magnitude is coincident with the increase of the in-phase and out-of-phase birefringence moduli, as seen in Figure 5, which indicates a departure from the rubbery plateau and an entrance into the glass transition regime.

Mechanical experiments were also performed at 1.5% strain. The dynamic mechanical shear stress data on polyisobutylene superimpose well for temperatures of 25, 35, and 45 °C. Figure 8 displays the normalized stress-optical coefficient obtained by dividing the birefringence amplitude by the shear-stress amplitude master curve. The data are normalized with respect to the low-frequency stress-optical coefficient. At low frequencies, this ratio is approximately 1; however, at strain frequencies above 10 s^{-1}, a frequency-dependent stress-optical relation is observed. This again is coincident with the increase in the absolute value of the asynchronous correlation intensity. Thus, the high-

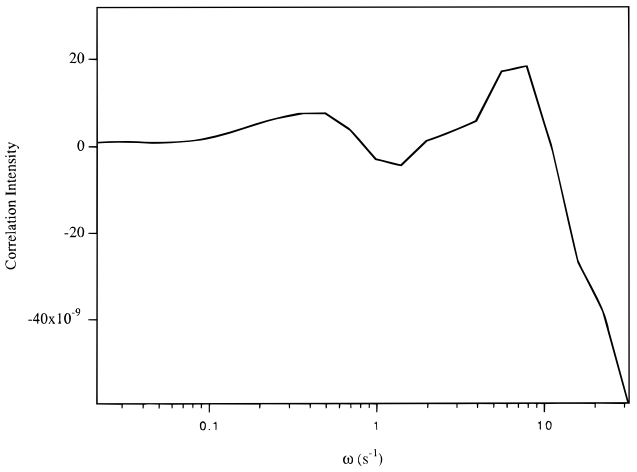

Figure 7. Asynchronous correlation intensity from the methyl side groups (2900 cm^{-1}) and the main chain (2926 cm^{-1}) vs frequency for 1.5% extension at room temperature.

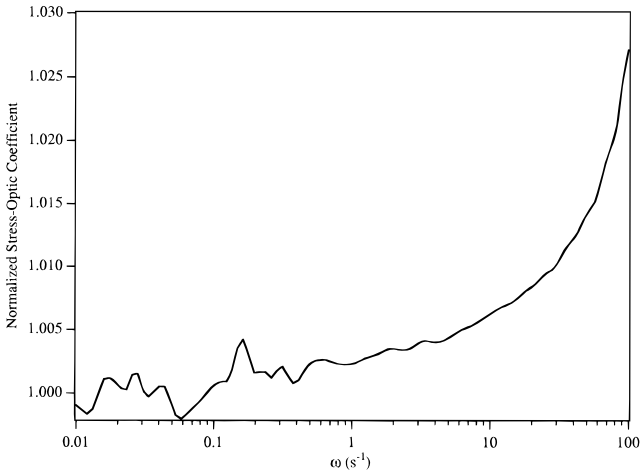

Figure 8. Normalized stress-optical coefficient vs frequency for 1.5% extension. Data are normalized by the low-frequency stress-optical coefficient.

frequency behavior of the stress-optical rule is a result of asynchronous motions between the main chain and side groups. Since these motions contribute the stress and birefringence differently, there no longer exists a frequency-independent proportionality.

5.0. Conclusions

Two-dimensional Raman scattering has been introduced for the study of polymer dynamics. Comparison to molecular models indicates that, for Gaussian chains, the dynamic Raman anisotropy is linearly related to the stress borne by a particular species. Additionally, simultaneous birefringence optics provide for the measurement of bulk rheology. It is shown that the birefringence and Raman anisotropy are proportional for the homopolymer polyisobutylene.

Cross correlation analysis enhances spectral resolution and offers insight into interspecies interactions. For polyisobutylene, the appearance of an asynchronous intensity indicates that the polymer backbone and side groups reorient differently as the mechanical glass transition is approached. This provides a molecular description of the observed frequency dependence of the stress-optical coefficient in this region.

Acknowledgment. The financial support of Eastman Kodak and the National Science Foundation, DMF

9120360, is gratefully acknowledged. Also, the valuable insight of Mr. Eric D. Carlson is appreciated.

References and Notes

(1) Ward, I. M. *Structure and Properties of Oriented Polymers*; Applied Science Publishers: London, U.K., 1975.
(2) Archer, L. A.; Fuller, G. G.; Nunnelley, L. *Polymer* **1992**, *33*, 3574.
(3) Archer, L. A.; Huang, K.; Fuller, G. G. *J. Rheol.* **1994**, *38* (4), 1101.
(4) Noda, I. *J. Am. Chem. Soc.* **1989**, *111*, 8116.
(5) Noda, I. *Appl. Spectrosc.* **1990**, *44* (4), 550.
(6) Ebihara, K.; Takahashi, H.; Noda, I. *Appl. Spectrosc.* **1993**, *47* (9), 1343.
(7) Gustafson, T. L.; Morris, D. L., Jr.; Huston, L. A.; Butler, R. M.; Noda, I. In *Time Resolved Vibrational Spectroscopy VI*; Lau, A., Siebert, F., Werncke, W., Eds.; Springer-Verlag: New York, 1994; p 131.
(8) Long, D. A. *Raman Spectroscopy*; McGraw-Hill: London, U.K., 1977.
(9) Bower, D. I. *J. Polym. Sci., Polym. Phys. Ed.* **1972**, *10*, 2135.
(10) Treloar, L. R. G. *The Physics of Rubber Elasticity*; *Monographs on the Physics and Chemistry of Materials*; Oxford University/Clarendon Press: Oxford, U.K., 1975.
(11) Jen, S.; Clark, N.; Pershan, P. S.; Priestley, E. B. *J. Chem. Phys.* **1977**, *66*, 4635.
(12) Kuhn, W.; Grün, F. *Kolloid Z.* **1942**, *101*, 248.
(13) Larson, R. G. *Constitutive Equations for Polymer Melts and Solutions*; Butterworths: Boston, 1988.
(14) Doi, M.; Edwards, S. *The Theory of Polymer Dynamics*; International Series of Mongraphs on Physics 73; Oxford University/Clarendon Press: Oxford, U.K., 1986.
(15) Horowitz, P.; Hill, W. *The Art of Electronics*; Cambridge University Press: New York, 1989.
(16) Koeing, J. L. *Appl. Spectrosc. Rev.* **1971**, *4* (2), 233.
(17) Seissler, H. W.; Holland-Moritz, K. *Infrared and Raman Spectroscopy of Polymers*; Marcel Dekker: New York, 1980.
(18) Bower, D. I.; Maddams, W. F. *The Vibrational Spectroscopy of Polymers*; Cambridge University Press: Cambridge, U.K., 1989.
(19) Marcott, C.; Dowrey, A. E.; Noda, I. *Appl. Spectrosc.* **1993**, *47* (9), 1324.

MA9507352